GEOPHYSICAL RESEARCH LETTERS, VOL. 28, NO. 5, PAGES 863-866, MARCH 1, 2001

Seismic anisotropy beneath the Lau back-arc basin inferred from sScS-ScS splitting data

Takashi Iidaka
Earthquake Research Institute, the University of Tokyo

Fenglin Niu
Carnegie Institution of Washington, DTM

Abstract. We determine upper mantle anisotropy just beneath active basins by comparing ScS and sScS waveform splitting. We have measured sScS-ScS shear-wave splitting with data from the SPANET and GSN seismic networks. The observed sScS-ScS shear-wave splitting suggests that there is a large lateral variation of anisotropy beneath the Lau back-arc basin. ScS- and sScS-waves which sample the southern part of the Lau basin show small splitting. In contrast, the northern part of the Lau basin, which is characterized to be tectonically active, is observed to have large seismic anisotropy with a WNW-ESE direction. The cause of anisotropy may be related to the mantle dynamics of the active basin.

Introduction

Shear-wave splitting analyses have provided us a new source of information to know the seismic structure and mantle dynamics. Seismic anisotropy within the upper mantle is often explained by strain-induced lattice preferred orientation in peridotite minerals [e.g., *Nicolas et al.*, 1973]. On the other hand, recent studies also showed that seismic anisotropy in the mantle wedge is closely related to partial melting in the same region [e.g., *Iidaka and Obara*, 1995].

Knowledge of the seismic structure beneath a back-arc spreading center is important to understand the dynamics of tectonic processes observed at earth's surface. Therefore, both tomographic and anisotropic studies are useful in order to answer such questions like whether the mantle upwelling beneath a spreading center is passive or active, and what kind of interaction exists between subduction and back-arc spreading. They are also essential to understanding the possible geochemical source of arc and back-arc magmas, and thus the origin of back-arc spreading. Most of the previous studies used SKS and S waves for the detection of anisotropic areas [e.g., *Bowman and Ando*, 1987; *Fischer and Wiens*, 1996]. Due to the source-station geometry it was very difficult to investigate the anisotropy just beneath a spreading center, simply because no seismic stations located above a spreading center is available.

ScS is an S wave reflected by the core-mantle boundary (CMB), sScS is an S wave reflected first by the earth's surface and then by the CMB. When the epicentral distance is very small the only difference between these two phases is the two-ways upper mantle ray paths from the source to the surface (inset of Fig. 1). In this study, we propose to compare differential waveform splitting between ScS and sScS to examine upper mantle anisotropy just beneath the active Lau back-arc basin.

Data

We use the broadband waveform data from the SPANET (South PAcific broadband seismic NETwork) and GSN networks (Fig. 1). The SPANET composed of 16 broadband stations deployed on oceanic islands at southern Pacific regions since the end of 1997. We use one station, AFI, which belongs to the GSN network of IRIS. A total of 8 large deep earthquakes occurred in the Fiji-Tonga subduction zone during the period from 1991 to 1998 are used (Fig. 1) The source parameters are obtained from Harvard CMT catalog.

Method

Shear-wave splitting is usually expressed by two parameters, the fast polarization azimuth ϕ (in degrees), and the time-lag τ (in seconds), which is

Paper number 2000GL012030.
0094-8276/01/2000GL012030$05.00

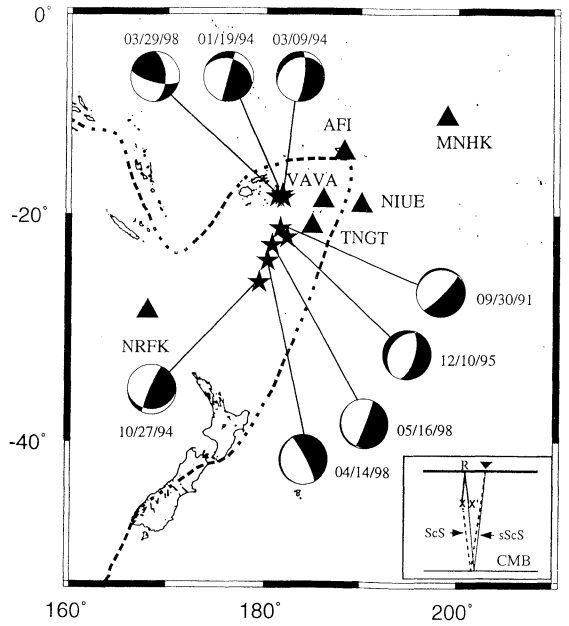

Fig. 1 Location map of the earthquakes (stars) and seismic stations (triangles) which belong to SPANET and GSN. The depths of the earthquakes are deeper than 400 km. Schematic ray paths of sScS and ScS are shown in the inset.

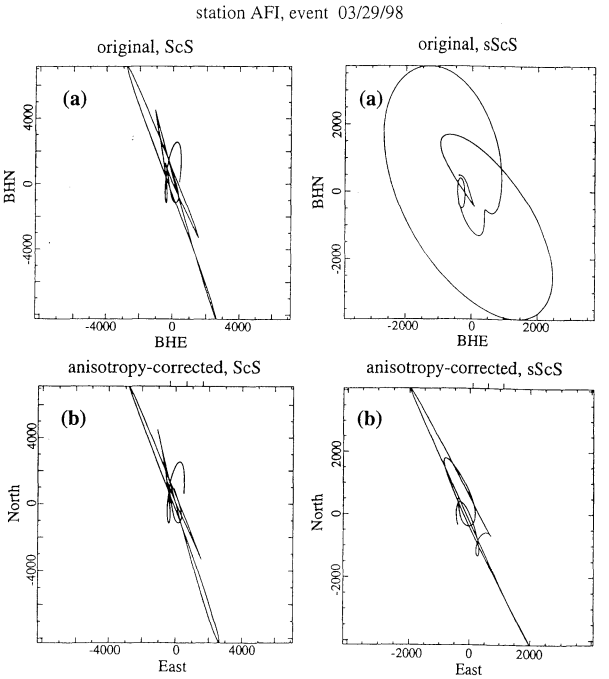

Fig. 3 Examples of particle motions of the ScS (left) and sScS (right) waves. Particle motions of the original and anisotropy-corrected waveforms are shown in *a)* and *b)*, respectively. See text for detailed explanation for anisotropy-corrected waveforms.

the delayed time between the fast and slow components of a shear wave. We use the same techniques as employed by *Fukao* [1984] to determine the shear-wave splitting. The horizontal components of broadband seismograms are first bandpass filtered at frequencies between 0.0125-0.04 Hz. We

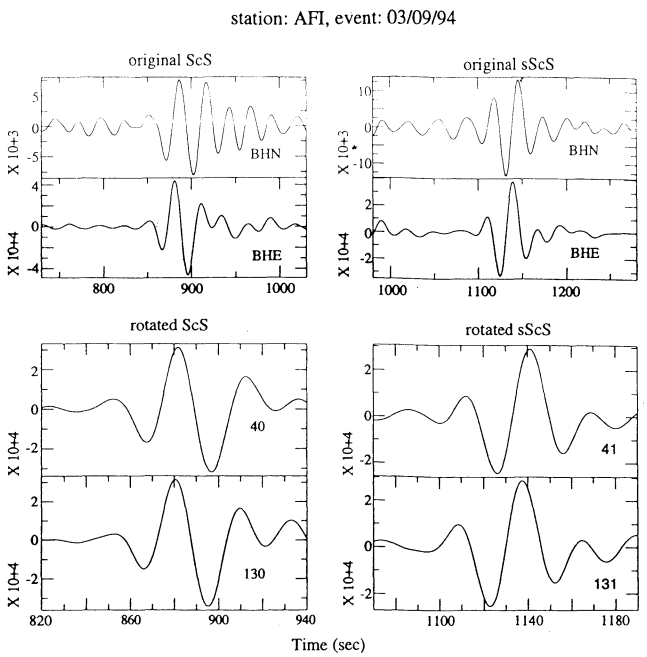

Fig. 2 Examples of the ScS (left) and sScS (right) waves. The original N-S, E-W components and the two components which have maximum cross-correlation are shown upper and lower, respectively.

then handpick ScS- and sScS-waves from individual seismograms. We calculated cross-correlation for the two horizontal seismogram components over a grid -90° to +90° for ϕ and window of 100 sec for τ with increments of 1° and 0.05 s, respectively. The time-lag τ (in seconds) and the fast polarization azimuth ϕ (in degree) are defined to be the values which yielded the maximum correlation (Fig. 2).

In order to confirm the resulted splitting parameters, ϕ and τ, we calculate anisotropy-corrected seismograms. As shown in Fig. 3, the anisotropy-corrected particle motion shows a linear orbit, as expected from the source mechanism.

RESULTS and DISCUSSION

According to the location of the surface bouncing point R of sScS (inset of Fig. 1), we divide the 8 earthquakes into two groups. The northern group (A) includes 3 earthquakes, which occurred at a latitude larger than −20°. The southern group (B) contains the other 5 earthquakes. As shown in Fig. 4, there is a remarkable difference of τ between the ScS- and sScS-waves for the northern group. We observe a large shear-wave splitting from the sScS-waves, and only a small τ from the ScS-wave. Polarization azimuths of sScS-

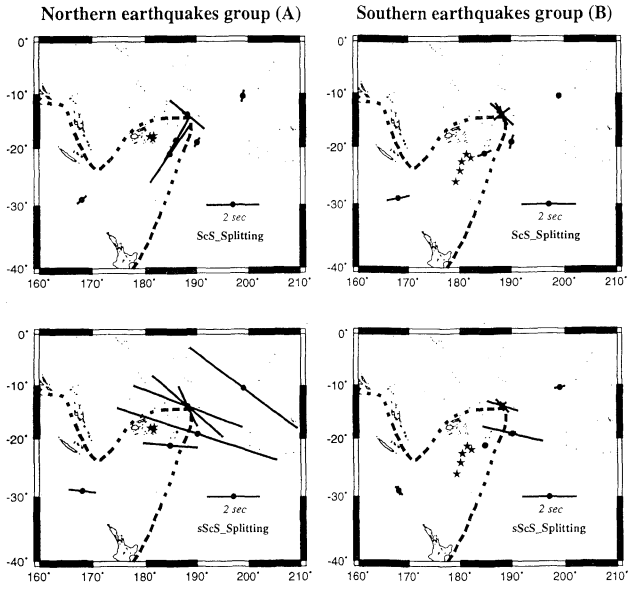

Fig. 4 Shear-wave splitting of ScS (upper figure) and sScS (lower figure) waves observed from the northern earthquake group (A) and the southern earthquake group (B). The hypocenters are shown by stars. ϕ and τ are shown by the direction and length of the bar, respectively.

wave among stations are roughly the same, with a direction of WNW-ESE. They are different from those of the ScS-waves, which exhibit a large variation among stations. On the other hand, both the sScS- and ScS-waves from the earthquakes of the southern group are only slightly split. Their fast directions are roughly NW-SE.

As shown in the inset of Fig. 1, the difference of shear-wave splitting between the ScS- and sScS-waves can only be attributed to the path XRX' of sScS, when epicentral distance is small. In Fig. 5, we show a map view of the ray path XRX'. These source-side upper mantle ray paths are located at the western part of the northern Lau basin for the northern group earthquakes, and are located around the western part of the southern Lau basin for the southern group earthquakes.

The observed differential τ values between the sScS- and ScS-waves, $\delta\tau_{sScS-ScS}$, from the northern group are approximately 2~6 sec. It is reasonable to assume that the amplitude of splitting accumulated by the anisotropy from ray paths XR and RX' is the same, which is a half of $\delta\tau_{sScS-ScS}$. Therefore, the mantle anisotropy beneath the western part of the northern Lau basin has a fast direction of WNW-ESE and will cause a 1~3 sec splitting for a vertical incident shear wave. In contrast, the anisotropy within the upper mantle beneath the western part of the southern Lau basin is very weak.

Although a detailed map of the shear-wave splitting in Tonga-Fiji regions was suggested by *Fischer and Wiens* [1996], anisotropy beneath the central part of the Lau basin is still unclear due to lack of seismic stations located within the Lau basin. This prevents us for a fully understanding of the dynamics of the active Lau basin. The fast polarization direction observed from the northern group is consistent with that of *Fischer and Wiens* [1996]. However, the estimated value of τ, 1~3 sec here, is almost twice as large as that observed by *Fischer and Wiens* [1996]. As the sampled regions of the two studies are not completely overlapped, this difference might suggest that large lateral variation of the anisotropy exists at the Lau basin. This inference is also consistent with our observation of a large difference between the northern and the southern groups. Similar frequency dependence of anisotropy for SKS and S waves was observed at New Zealand by *Marson-Pidgeon and Savage* [1997] because of similar possible reasons.

The cause of the anisotropy is generally interpretated by two models; the olivine alignment model and the crack alignment model [e.g., *Crampin*, 1981]. Mantle anisotropy observed in most regions can be explained by olivine alignment, and is caused by mantle flow. There are, however, some observations [e.g., *Iidaka and Obara*, 1995]

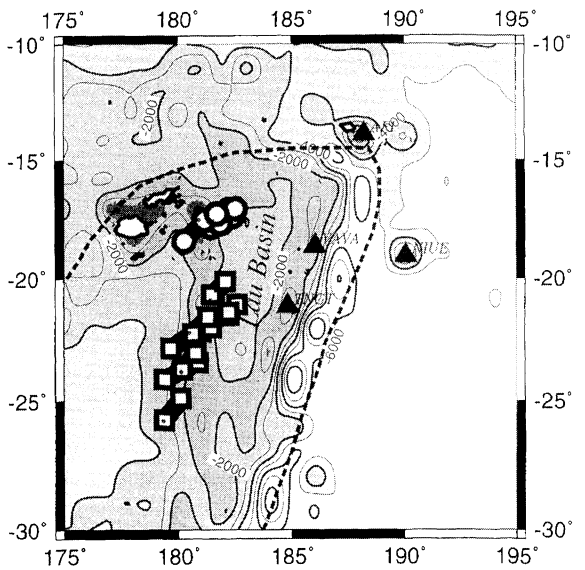

Fig. 5 Map view of the residual ray paths XRX' of sScS shown in the inset of Fig. 1. Ray paths from northern and southern earthquakes are shown by circle-bar and square-bar, respectively. Contours denote bathymetry with an interval of 2000 m.

that suggest anisotropy within a mantle wedge is caused by rising magma, rather than mantle flow. We suggest that the strong anisotropy observed beneath the western part of the northern Lau basin, might be also caused by melt filled cracks, since the strong anisotropic region observed here happens to be a region with extremely low-velocity [e.g., *Zhao et al.*,, 1997] and low-Q [e.g., *Barazangi and Isacks*, 1971; *Roth et al.*, 1999]. If the anisotropic region is caused by olivine alignment, a zone of extremely low-Q and low-velocity would not be found. The northern Lau basin is also characterized to be geologically active [e.g., *Hawkins*, 1995]. The cause of the anisotropic region beneath the Lau basin might reflect the rising magma beneath the active back-arc basin.

Normally crack-induced anisotropy is expected to yield fast directions parallel to the maximum principal stress direction. In the Lau basin, Central Lau spreading center extends along the N-S direction and is opened in the E-W direction. Most models of rifted regions suggest that stress should be extensional, with the maximum horizontal stress parallel to the rift. The direction of maximum horizontal stress (N-S) therefore seems to be inconsistent with our results. However, the observed large anisotropic region is just beneath Peggy ridge which is trending to the NW-SE direction. At the Peggy ridge, a spreading model with an open direction of NE-SW was proposed by *Scalter et al.*, [1972]. The spreading center with a NW-SE strike might have deep roots that extends to the depths of several hundred kilometers. As the result, a NW-SE fast polarized anisotropic region is seismologically observed. Further detailed maps of polarization directions will reveal the dynamic processes that control the spreading of the Lau basin.

Conclusion

We have detected a strong anisotropic region within the tectonically active Lau back-arc basin by comparing the waveform splitting between sScS and ScS. Previous studies suggest that the same region is also characterized by extremely low-velocity and low-Q. All these seismological studies support the idea that a region of partial melt exists beneath the active basin.

Acknowledgments. Seismic Analysis Code (SAC) was used in our calculations. We thank for Dr. Suetsugu, Dr. Kanjo, Dr. Inoue and Dr. Sekiguchi for providing us with the SPANET data. The bathymetry data was provided by NOAA. This research was supported by grants. We thank Dr. Kaneshima for helpful discussions. We thank Dr. Aurnou for critically reading the manuscript, and two anonymous reviewers for constructive reviews.

References

Barazangi, M., and B. Isacks, Lateral variation of seismic-wave attenuation in the upper mantle above the inclined earthquake zone of the Tonga Island Arc: Deep anomaly in the upper mantle, *J. Geophys. Res.*, *76*, 8493-8516, 1971.

Bowman, J.R., and M. Ando, Shear-wave splitting in the upper-mantle wedge above the Tonga subduction zone, *Geophys. J. R. astr. Soc.*, *88*, 25-41, 1987.

Crampin, S., A review of wave motion in anisotropic and cracked elastic-medium, *Wave Motion*, *3*, 343-391, 1981.

Fischer, K.M., and D.A. Wiens, The depth distribution of mantle anisotropy beneath the Tonga subduction zone, *Earth Planet. Sci. Lett.*, *142*, 253-260, 1996.

Fukao, Y., Evidence from core-reflected shear waves anisotropy in the Earth's mantle, *Nature*, *309*, 695-698, 1984.

Hawkins, J.W., The Geology of the Lau Basin, in *Backarc Basins: Tectonics and Magmatism* edited by B. Taylor, pp. 63-138, 1995.

Iidaka, T., and K. Obara, Shear-wave polarization anisotropy in the mantle wedge above the subducting Pacific plate, *Tectonophys.*, *249*, 53-68, 1995.

Marson-Pidgeon, K., and M. Savage, Frequency-dependent anisotropy in Wellington, New Zealand, *Geophys. Res. Lett.*, *24*, 3297-3300, 1997.

Nicolas, A., F. Boudier, and A.M. Boullier, Mechanism of flow in naturally and experimentally deformed peridotites, *Am. J. Sci.*, *273*, 853-876, 1973.

Roth, E.G., D.W. Wiens, L.M. Dorman, J. Hildebrand, and S.P. Webb, Seismic attenuation tomography of the Tonga-Fiji region using phase pair methods, *J. Geophys. Res.*, *104*, 4795-4809, 1999.

Sclater, J.G., J.W. Hawkins, J. Mammerckx, and C.G. Chase, Crustal extension between the Tonga and Lau Ridges: Petrologic and Geophysical evidence, *Geol. Soc. Am. Bull.*, *83*, 505-518, 1972.

Zhao, D., Y. Xu, D.A. Wiens, L. Dorman, J. Hilebrand, and S. Webb, Depth extent of the Lau back-arc spreading center and its relation to subduction processes, *Science*, *278*, 254-257, 1997.

Takashi Iidaka ERI,the University of Tokyo, 1-1-1 Yayoi, Bunkyo-ku, Tokyo 113-0032, Japan. (e-mail iidaka@eri.u-tokyo.ac.jp) Fenglin Niu, Carnegie Institution of Washington, DTM, U.S.A. (e-mail niu@dtm.ciw.edu)

(received July 11, 2000; revised October 20, 2000; accepted October 25, 2000.)